Inelastic-neutron-scattering studies of a quasi-one-dimensional charge-density-wave system: Characterization of interchain interactions

J-F. Bardeau* and A. Bulou
Laboratoire PEC, Université du Maine, 72085 Le Mans Cédex, France

B. I. Swanson
CST-1, MS J565, LANL, Los Alamos, New Mexico 87545

B. Hennion
LLB, CEN Saclay, 91191 Gif/Yvette Cédex, France

(Received 27 January 1998)

The low-frequency part of the phonon spectrum of perdeuterated-$[Pt(en)_2][Pt(en)_2I_2](ClO_4)_4$ (where en = 1,2-diaminoethane) has been measured by inelastic neutron scattering. Longitudinal optical branches quasi-parallel to the acoustic ones are observed along the $[\xi 00]$ and $[0\xi 0]$ directions, revealing the existence of a weak coupling of the PtI charge-density-wave chains with their environment. The whole data, obtained in the (a^*,b^*) reciprocal plane, are well described by a two-dimensional model that allowed the determination of the coupling constant and gaps for the $q=0$ wave vector. The linear temperature dependence of the phonon energies indicates an increase in interchain interactions on cooling. [S0163-1829(98)04329-X]

I. INTRODUCTION

Over the past few years, numerous studies have been devoted to the $[M(L\text{-}L)_2][M(L\text{-}L)_2X_2]Y_4$ compounds where M represents a mixed-valence metal (Pt, Pd, Ni), X a halogen (Cl, Br, I), $(L\text{-}L)$ a bidentate ligand (such as 1,2-diaminoethane, 1,2-diaminopropane) and Y a counterion (ClO_4^-, I^-). The interest in these materials mainly comes from the existence of a quasi-one-dimensional MX sublattice in which the charge disproportionation δ of the metal ($M^{3-\delta}/M^{3+\delta}$) can be tuned from 0 to 1, and where various photoinduced polaronic defects have been observed.[1,2] The electronic properties of such systems and their defects have been well described by Peierls-Hubbard models.[3,4] Moreover, as these charge-density-wave (CDW) chains are strictly linear, good descriptions of the longitudinal vibrations were obtained with one-dimensional models, both for the perfect system and for those with electronic and isotopic defects.[5–7]

Clark[8] has shown that the ligands and counterions could modify the CDW sublattice and therefore the physical properties of the compounds. We have recently studied the relationship between the various measures of the CDW strength in MX systems and have shown that the electron-electron, electron-phonon coupling is largely controlled by the separation between the Pt atoms.[9] Recent structural analysis and Raman scattering studies[10] describe different structures for the protonated and perdeuterated (usually referred to as D-PtI) forms of $[Pt(en)_2]Pt(en)_2I_2](ClO_4)_4$ with existence of two types of chains, one of which is ordered in the halide positions and one of which is disordered, distinguished by a slight difference in charge disproportionation. Such a result suggests that the ordering of the CDW chains could be influenced by changes in the hydrogen bonding network that couples the MX chains to the environment.

This work reports on the investigations of the low-frequency part of the phonon spectrum of D-PtI by inelastic neutron scattering in order to provide signatures for interchains (i.e., chain-chain and chain-environment) interactions. It must be pointed out that recent studies of the D-PtI have shown the existence of a phase transition in the vicinity of 160 K (Ref. 11) associated with an ordering of the 1,2-diaminoethane, a transformation never previously mentioned in the hydrogenated form,[12] in spite of investigations. Therefore, with regard to the complex structure of the compound, we have studied D-PtI at 180 K in the high symmetry phase and proposed an average structure, assuming a weak charge disproportionation (Fig. 1). According to the positions of platinum and iodine in the unit cell, this latter is in fact similar to the one proposed by Endres[13] for the protonated form of PtI at room temperature.

II. EXPERIMENT

Several fully deuterated single crystals have been synthesized at Los Alamos National Laboratory. They look similar to golden plates with the a axis normal to the large face. The

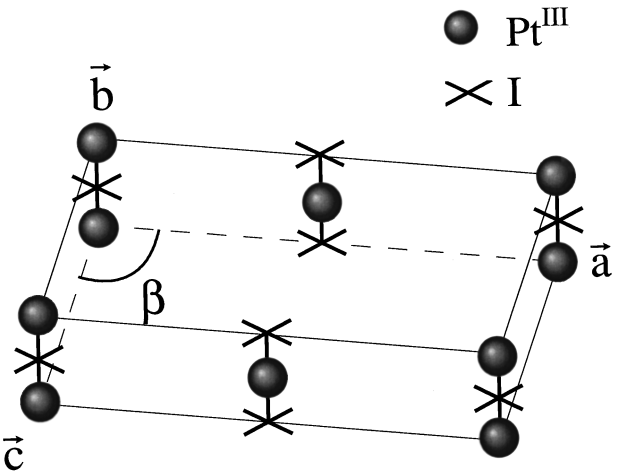

FIG. 1. Platinum and iodine positions in the average unit cell of $[Pt(en)_2][Pt(en)_2I_2](ClO_4)_4$ with the space group $C2/m$.

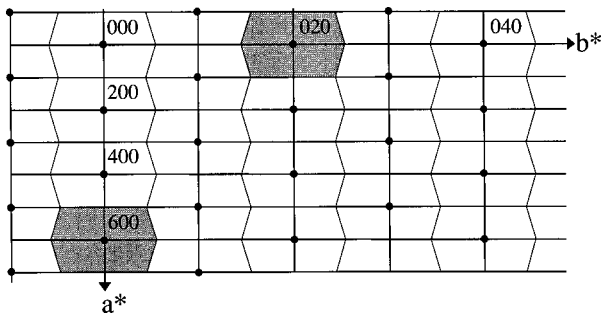

FIG. 2. The (a^*,b^*) reciprocal plane with evidence (highlighted) of the first Brillouin zone.

two biggest crystals have been assembled yielding a total volume close to 300 mm^3 with a mosaic spread of about 0.4°. They were set in an aluminum container filled with helium in order to avoid a possible exchange of deuterium with hydrogen and increase the thermal exchange. The experiments were carried out on the triple-axis spectrometer 4F1 of the LLB (Saclay, France) that operates with a cold neutron beam and is equipped with pyrolytic graphite monochromators (double monochromators) and analyzer. The measurements were performed with a fixed scattered wave vector $k_f = 2.662$ Å^{-1}, and a graphite filter located in front of the analyzer to suppress any higher-order contamination. Fixed scattered wave vectors $k_f = 1.64$ Å^{-1} and $k_f = 1.48$ Å^{-1} were also used when higher resolution was necessary. In all cases, the monochromators and analyzer were set flat in order to keep a good q resolution.

The experiments were done in the (a^*,b^*) reciprocal plane (Fig. 2) with the sample placed in a cryocooler. The dispersion curves from 0 to 8 meV were measured at 180 K, a temperature for which the thermal vibrations are reduced but where the crystal still exhibits the high symmetry phase. This study was complemented by measurements as a function of temperature in the vicinity of the zone center (along b^*) and at the zone boundary along a^*.

The inelastic-neutron-scattering spectra were refined with a program from the LLB accounting for the instrumental resolution and using a locally linear dispersion for phonons described as damped harmonic oscillators. This yields the peak positions as well as the dependence of intensities and linewidths along a given direction.

III. RESULTS

The measured phonon dispersion curves along the $[0\xi 0]$ and $[\xi 00]$ directions at 180 K are given in Fig. 3. The dispersion along the $[0\xi 0]$ direction (parallel to the chains) appears larger than along the $[\xi 00]$ one; such a result is consistent with the quasi-one-dimensional character of these materials. In both longitudinal cases (Fig. 4), one observes an optical branch that mimics an acoustic branch and hence will be called hereinafter pseudoacoustic. Figure 5 shows examples of scans with fixed scattered wave vectors which allow an appreciation of the quality of the spectra and the clarity of the acoustic branches and their resolution with respect to the pseudoacoustic ones. At the center of the Brillouin zone, it has not been possible to resolve the frequencies of the pseudoacoustic branches from the intense neighboring elastic signal. However, from the experimental q-wave vector dependence and from the model presented in the next section, the gap frequency for $q=0$ can be estimated at 0.12 meV (30 GHz) and 0.35 meV along the $[0\xi 0]$ and $[\xi 00]$ directions, respectively.

As shown below, the existence of these gaps reflects the presence of several weakly interacting sublattices. Therefore, in order to probe the evolution of these interactions, measurements as a function of temperature have been done at the

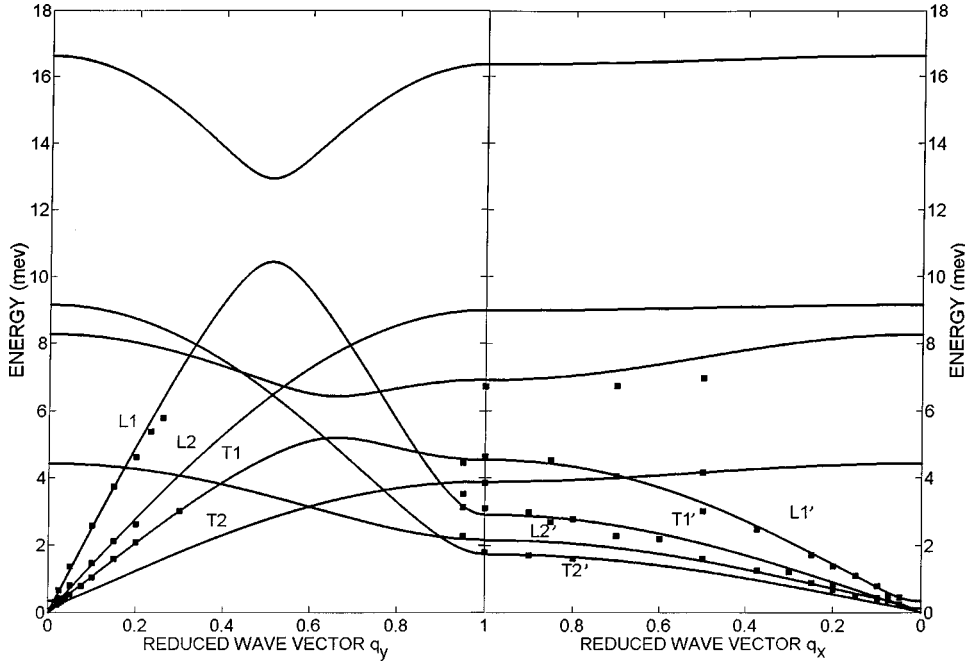

FIG. 3. Experimental (square) and calculated (full line) longitudinal (L) and transversal (T) dispersion curves at 180 K along the $[0\xi 0]$ and $[\xi 00]$ directions. The calculated phonon dispersion curves are performed with the two-dimensional model corresponding to the schematization given in Fig. 8.

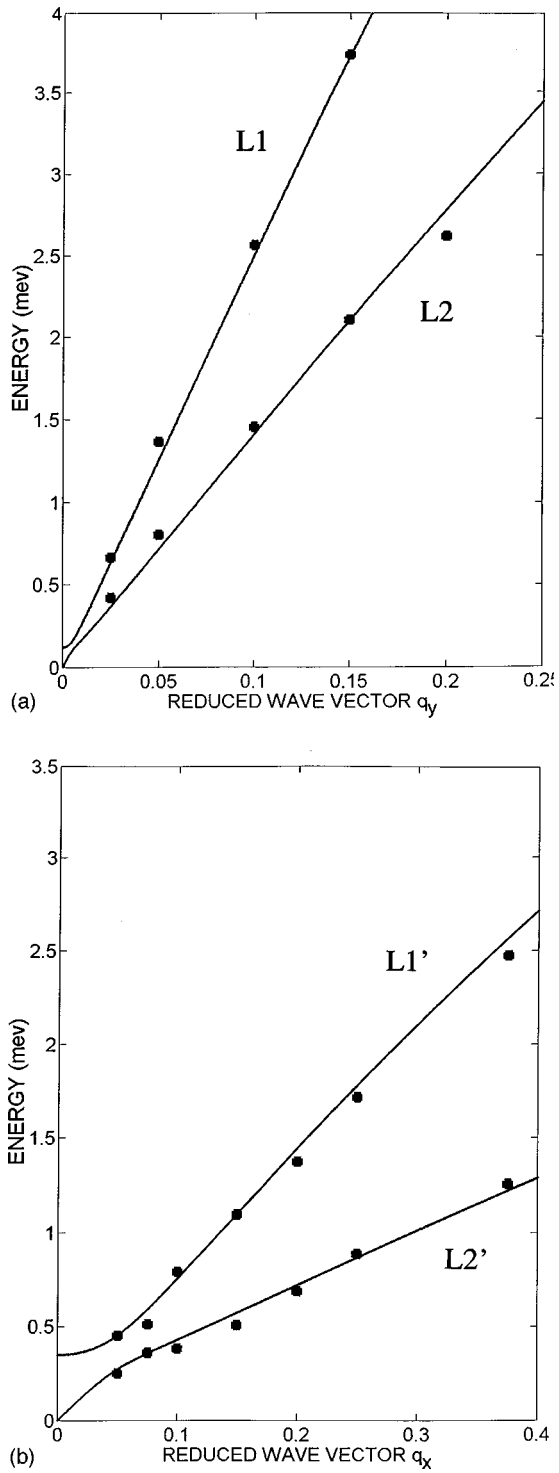

FIG. 4. Experimental and calculated (full line) longitudinal dispersion curves at 180 K along the [0ξ0] (a) and [ξ00] (b) directions. The calculations are performed with the two-dimensional model corresponding to the schematization given in Fig. 8.

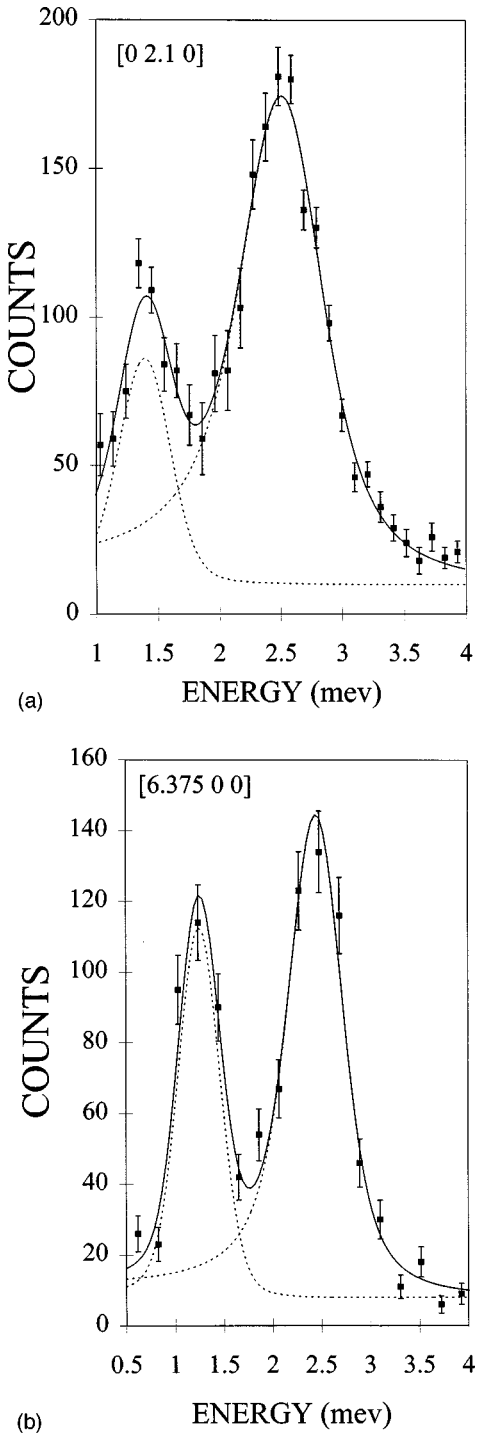

FIG. 5. Energy scans at 180 K (a) along the [0ξ0] direction ([0 2.1 0] Q point) and (b) along the [ξ00] direction ([6.375 0 0] Q point).

q point along the [0ξ0] direction where the intensities of acoustic and pseudoacoustic branches are of the same magnitude and well resolved (ξ=0.05). As appears in Fig. 6, there is a weak, but significant temperature dependence.

An investigation of the phonon spectrum at the boundary of the Brillouin zone along a^* has been also undertaken since the modes of PtI chains (see next section) could be affected by the chain-to-chain couplings. Figure 7 shows that the phonon energies increase linearly on cooling and the temperature sensitivity is stronger than the one at the center of the Brillouin zone (Fig. 6).

IV. DISCUSSION

First, let us point out that the Pt-I chains are parallel to the b axis, and that the monoclinic angle is β. Hence, the [0ξ0] direction is parallel to the chain axis, and the [ξ00] direction is strictly normal to it. Therefore, the present results obtained

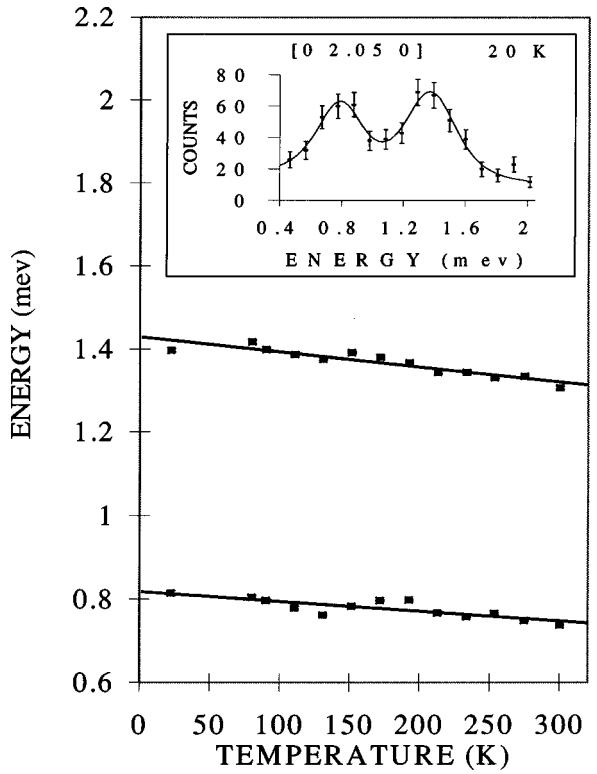

FIG. 6. Temperature dependence of the acoustic and pseudoacoustic phonons at the [0 2.05 0] Q point. The inset represents an example of energy scan at 20 K.

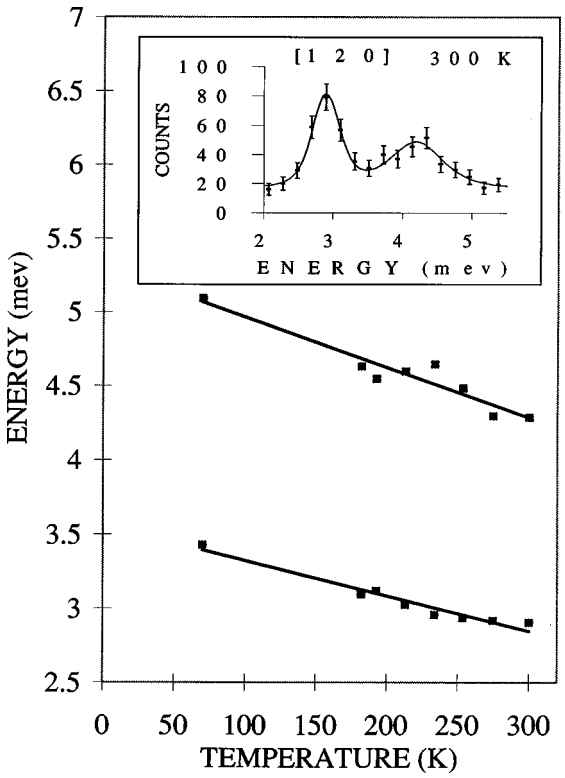

FIG. 7. Temperature dependence of the low-energy phonons at the [1 2 0] Q point. The inset represents an example of energy scan at 300 K.

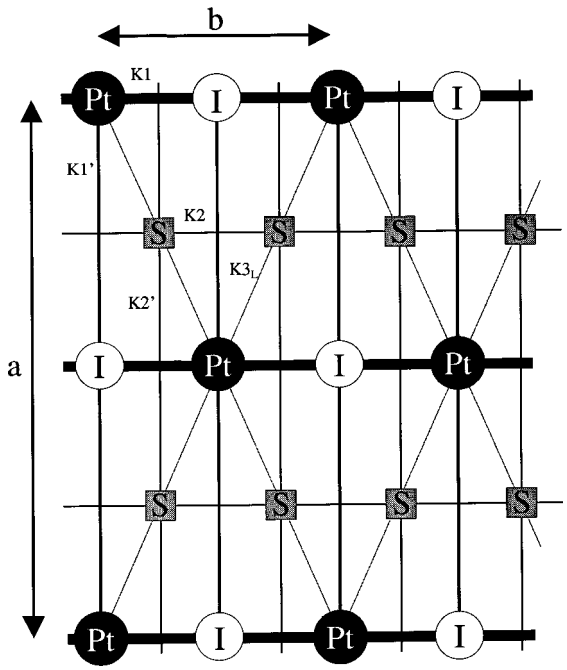

FIG. 8. Schematic representations and labeling of the force constants of a simplified two-dimensional model in the (a,b) plane. Each of the $K1$, $K2$, $K1'$, $K2'$ interactions are characterized by two force constants, one parallel to the bond (subscript L) and the other perpendicular to the bond (subscript T).

in the neighborhood of [0 2 0] and [6 0 0] (or [4 0 0] depending on the scattered wave vector) provide reliable longitudinal and transversal data.

The presence of a pseudoacoustic branch along both the $[0\xi 0]$ and $[\xi 00]$ directions can be explained by the existence of two weakly interacting systems. In the former case, with regard to the lattice dynamics results obtained in the framework of a one-dimensional model [5-7], one of these systems can be identified as the Pt-I chains; the second one may be the organic molecules, perchlorate, or both. On the other hand, the existence of a similar behavior (but less marked) along the $[\xi 00]$ axis cannot be so easily explained.

In order to explain the whole dispersion curves and the pseudoacoustic gaps at the zone center, we have used a model of the (a,b) plane (Fig. 8) that builds on the structural features of this material[11] and the weakness of the charge disproportionation. This explicitly contains platinum and iodine atoms, but the environment is represented by a phenomenological atom S. The former are considered with their real masses while the mass of the S atoms is chosen as the average of the organic and the ClO_4 molecules. The model involves the force constants shown in Fig. 8 for the Pt-I and S-S interactions, each one characterized by a component parallel and perpendicular to a given pair of atoms (and labeled with subscripts L and T, respectively).[14] In addition, a single force constant ($K3_L$) has been introduced to couple the two systems.

The results drawn in Fig. 3 were obtained with the values given in Table I. According to this model which fits the experimental data well, general rules can be deduced about the relative magnitude of the various force constants. Let us remark that $K3_L$ is almost 3000 times smaller than the $K1_L$ and 450 times smaller that the $K2_L$. This indicates the pres-

TABLE I. Calculated force constants used in the two-dimensional model described in Fig. 8.

Pt-I interactions (Nm^{-1})		S-S interactions (Nm^{-1})		Pt-S interaction (Nm^{-1})
$K1_L=39.5$	$K1_T=6.8$	$K2_L=6.2$	$K2_T=1.15$	$K3_L=0.014$
$K1'_L=3.3$	$K1'_T=1.3$	$K2'_L=0.35$	$K2'_T=0.23$	

ence of ''hard'' Pt-I chains along the b axis and a very weak coupling with the S atoms. The magnitude of the force constants between the Pt and I atoms along the a axis are at least 12 times smaller than along b which is realistic with regard to the relative interatomic distances (Fig. 8).

The calculated low-frequency spectra for the longitudinal modes along the b axis are represented in Fig. 4(a) together with the experimental results; the so-called ν_1 (Raman active mode of the PtI chain) and ν_3 (infrared active mode of the PtI chain) at 14 meV (Ref. 15) and 11 meV (Ref. 16) or 10.8 meV (Ref. 15) are calculated at 13 and 10.5 meV, respectively. It appears, as expected, that along this direction, the acoustic and pseudoacoustic branches mainly correspond to displacements of a single system, the S sublattice for the former, and the Pt-I chains for the latter. For small q vectors, there is of course a strong mixing resulting from the anticrossing of the branches. The gap is calculated at 0.12 meV (at 180 K) and the normal coordinate vibrations for this optical mode are shown in Fig. 9.

The calculations show that the energies of the two gaps at the center of the Brillouin zone along the $[0\xi0]$ and $[\xi00]$ are mainly driven by the $K3_L$ force constant (note that these energies are different just because the interatomic distances are different along the a and b axes; in a cubic lattice these modes would be degenerate). The model shows that the slight increase, on cooling, of the frequency of the pseudoacoustic mode at the (0 2.05 0) point (Fig. 6) reflects a similar behavior of the gap energy at the center of the Brillouin zone. It corresponds to an increase of the $K3_L$ force constant.

A change in the properties of the CDW system should also have some effect on the frequencies of several modes. For example, it is easy to see that variation of the platinum charge disproportionation would change the chain-to-chain coupling (schematized by dashed lines in Fig. 9, but not explicitly introduced in the model) and so lead to a modification of the phonon energies characteristic of the PtI chain at the boundaries of the Brillouin zone (where the platinum of nearest-neighbor chains move in opposite directions). Otherwise, let us point out that this interaction cannot influence the magnitude of the gap at the center of the Brillouin zone since this latter does not couple the two systems (Fig. 9, left). Therefore, several investigations have been performed at the boundaries of the Brillouin zone as a function of temperature, and Fig. 7 shows an example of an energy scan at the (1 2 0) Q point together with its temperature dependence. With regard to the calculated dispersion curves obtained along the $[\xi00]$ direction, the phonon energies in the vicinity of 3 and 4.5 meV are attributed to the transversal and longitudinal modes of the PtI chains, respectively (Fig. 3). According to the present data, a linear variation of the phonon energies appears on cooling and the higher energy one is more sensitive to temperature than the other (Fig. 7). In the framework of the model, such a behavior could be explained by an increase of the $K1'_L/K1'_T$ ratio. As discussed above, this can be the consequence of variations of the chain-to-chain interaction possibly due to change in the properties of the CDW system. However, with regard to the complexity of the system, it cannot be excluded that another phenomenon be at the origin of the effect, such as, for example, the fairly large variations of the a parameter, as observed by neutron diffraction.[11] The sensitivity of the method would be better checked by studying a system exhibiting the Peierls transition.

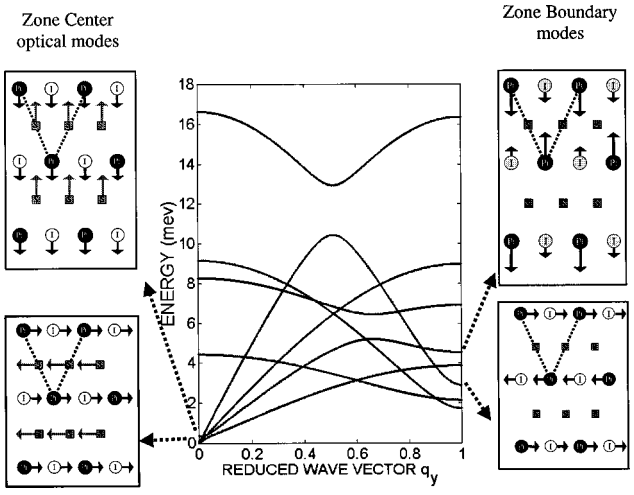

FIG. 9. Normal coordinates of vibrations of the pseudoacoustic modes at the zone center of the Brillouin zone (left) and of the modes characteristic of the Pt-I chains at the boundary of the Brillouin zone (right).

V. CONCLUSION

These investigations of the low-frequency dispersion curves of $[Pt(en)_2][Pt(en)_2I_2](ClO_4)_4$ along the $[0\xi0]$ and $[\xi00]$ directions reveal the existence of longitudinal pseudoacoustic branches, which reflect the presence of two weakly interacting systems, one of them being the Pt-I chains. Calculations in the framework of a realistic two-dimensional model made it possible to deduce that the gaps of the longitudinal pseudoacoustic branches at the zone center are directly proportional to the chain-environment coupling constant. It can be noted that with regard to their frequency range (30 and 85 GHz) the gaps could be directly measured using a Brillouin spectrometer. The investigations of the phonon spectrum both at the center and boundaries of the Brillouin zone show linear variations of the phonon energy on cooling. It appears from the model that a slight increase of the chain-environment interaction and the introduction of a chain-chain coupling can explain the temperature behavior of the phonon energies. Further studies in another reciprocal plane could be promising since the observation of a pseudoa-

coustic branch along c^* would allow us to identify undoubtedly the second system, presumably as the perchlorate: this interpretation seems already reasonable with regard to the particular position of this system in the model.

These investigations by inelastic neutron scattering show that good quality data can be expected in spite of the complexity of the compounds and of their phonon spectra. This work allowed the characterization of interchain interactions and the introduction of a model to appreciate the order of magnitude of interactions which could be elaborated in further theoretical studies. However, further comparative investigations seem to be necessary for a more precise determination of the relationship between the evolution of chain-chain and chain-environment interactions, the CDW sublattice, and the physical properties of the material. Such studies could also be helpful for understanding the theoretical stability or the relaxation processes of photoexcited states in this complex.[17–20]

*Present address: CST-1, MS G755, LANL, Los Alamos, NM 87545.

[1] S. Kurita, M. Haruki, and K. Miyagawa, J. Phys. Soc. Jpn. **57**, 1789 (1988).

[2] R. J. Donohoe, S. A. Ekberg, C. D. Tait, and B. I. Swanson, Solid State Commun. **71**, 49 (1989).

[3] D. Baeriswyl and A. R. Bishop, J. Phys. C **21**, 339 (1988).

[4] K. Nasu and A. Mishima, Rev. Solid State Sci. **2**, 539 (1988).

[5] A. Bulou, R. J. Donohoe, and B. I. Swanson, J. Phys.: Condens. Matter **3**, 1709 (1991).

[6] S. P. Love, L. A. Worl, R. J. Donohoe, S. C. Huckett, and B. I. Swanson, Phys. Rev. B **46**, 813 (1992).

[7] J-F. Bardeau, A. Bulou, and B. I. Swanson, J. Raman Spectrosc. **26**, 1051 (1995).

[8] R. J. H. Clark, Adv. Infrared Raman Spectros. **11**, 95 (1984).

[9] B. Scott, S. P. Love, G. S. Kanner, S. R. Johnson, M. Berkey, B. I. Swanson, A. Saxena, X. Z. Huang, and A. R. Bishop, J. Mol. Struct. **356**, 207 (1995).

[10] B. Scott, B. L. Bracewell, S. R. Johnson, J-F. Bardeau, A. Bulou, and B. Hennion, Chem. Mater. **8**, 321 (1996); G. Strouse, B. Scott, B. I. Swanson, A. Saxena, I. Batostoc, J. T. Gammel, and A. R. Bishop, Chem. Phys. Lett. (to be published).

[11] J-F. Bardeau, A. Bulou, W. T. Klooster, T. F. Koetzle, S. Johnson, B. Scott, B. I. Swanson, and J. Eckert, Acta Crystallogr., Sect. B: Struct. Sci. **52**, 854 (1996).

[12] K. Toriumi, M. Yamashita, S. Kurita, I. Murase, and T. Ito, Acta Crystallogr., Sect. B: Struct. Sci. **49**, 497 (1993).

[13] H. Endres, H. J. Keller, R. Martin, H. Nam Gung, and U. Traeger, Acta Crystallogr., Sect. B: Struct. Crystallogr. Cryst. Chem. **35**, 1885 (1979).

[14] M. Born and K. Huang, *Dynamical Theory of Crystal Lattices* (Oxford University Press, Oxford, 1956).

[15] S. P. Love, L. A. Worl, R. J. Donohoe, S. C. Huckett, S. R. Johnson, and B. I. Swanson, Synth. Met. **55-57**, 3456 (1993).

[16] L. Degiorgi, P. Wachter, M. Haruki, and S. Kurita, Phys. Rev. B **42**, 4341 (1990).

[17] H. Okamoto, T. Mitani, K. Toriumi, and M. Yamashita, Phys. Rev. Lett. **69**, 2248 (1992).

[18] M. Suzuki, K. Nasu, and M. Okazaki, Phys. Rev. B **45**, 1605 (1992).

[19] H. Okamoto, Y. Oka, T. Mitani, K. Toriumi, and M. Yamashita, Mol. Cryst. Liq. Cryst. Sci. Technol., Sect. A **256**, 161 (1994).

[20] A. Mishima, Synth. Met. **70**, 1197 (1995).